Plant Physiology and Biochemistry 135 (2019) 233–241

Contents lists available at ScienceDirect

Plant Physiology and Biochemistry

journal homepage: www.elsevier.com/locate/plaphy

Research article

Occurrence of internal browning in tuberous roots of sweetpotato and its related starch biosynthesis

Nobuyuki Fukuoka[a,*,1], Masahiro Miyata[a,1], Tatsuro Hamada[b], Eishin Takeshita[c]

[a] Experimental Farm, Ishikawa Prefectural University, 1-308, Suematsu, Nonoichi, Ishikawa, 921-8836, Japan
[b] Research Institute for Bioresources and Biotechnology, Ishikawa Prefectural University, 1-308, Suematsu, Nonoichi, Ishikawa, 921-8836, Japan
[c] Ishikawa Sand Dune Agricultural Research Center, 5-2, Uchihisumi, Kahoku, Ishikawa, 929-1126, Japan

ARTICLE INFO

Keywords:
Browning
Gene expression
Ipomoea batatas
Polyphenol biosynthesis
ROS generation
Starch grain

ABSTRACT

Although sweetpotato is an important crop worldwide, there has been almost no research on the occurrence of internal browning (IB) to date. In this study, we clarified the mechanism of occurrence of the disorder by using two types of cultivars with different IB susceptibility. In cells around the secondary vascular tissue, large size of starch grains accumulated in IB-susceptible cultivar compared with resistant one. Histochemical observation performed on cells around the secondary vascular tissues showed the presence of high levels of polyphenol oxidase activity, chlorogenic acid, and hydrogen peroxide in cells from the IB-affected regions in IB-susceptible cultivar. Likewise, high levels of starch content, hydrogen peroxide concentration, and polyphenol content were detected in the affected regions of IB-susceptible cultivar. In IB-susceptible cultivar, both the transcript levels of gens related starch and polyphenol biosynthesis were higher at an early stage of root maturation, while the levels in resistant cultivar were low at this stage and thereafter increased relatively more moderately. These observations suggest that the occurrence of IB disorder in sweetpotato largely depends on the morphology and timing of accumulated starch grain in cells around the secondary vascular tissues.

1. Introduction

Internal browning (IB) of sweetpotato (*Ipomoea batatas*) characterised by an abnormal brown colouration inside the tuberous root is a physiological disorder found in the mature phase of the root (Fig. 1). Since IB cannot be detected by examination of external appearance, affected sweet potato tubers are often put on the market. IB causes the sweetpotato to have reduced storage stability and affects the taste. So, the sweetpotato having this disorder causes consumers to discard. Although sweetpotato is an important crop worldwide, research on IB in this crop remains limited to its relationship to growth conditions, and only a few reports have been published (Fujita et al., 2000; Fukuoka et al., 2009).

Recently, we reported that IB damage of sweetpotato initially occurs in cells around the secondary vascular tissue and that cells in this region have a higher area per cell occupied by starch grains compared to the normal region (Fukuoka et al., 2018). Furthermore, increased concentration of reactive oxygen species (ROS) and active polyphenol biosynthesis can be found in IB-damaged regions compared to the normal regions. From these findings, we consider that high ROS generation induced by active starch biosynthesis leads to membrane deterioration followed by disrupted cellular integrity resulting in the accumulation of brown pigments. Intervarietal differences with respect to the severity of IB disorder are well known (Fujita et al., 2000), but until recently, the physiological mechanism behind this phenomenon has not been known. Detailed investigation of the intervarietal differences in IB occurrence should serve to clarify the mechanisms of the occurrence of this disorder.

In *Raphanus* roots, the accumulation of ROS in root tissues accelerated the loss of cellular integrity, resulting in the accumulation of brown pigments (Fukuoka and Enomoto, 2001, 2002). According to Fukuoka et al. (2014), cell disruption induced by high concentration of ROS differs among radish cultivars, and cultivars with large amounts of protopectin content are less susceptible to cell breakdown, even under high concentrations of ROS. Likewise, in pear fruit, increased depolymerisation of pectic polysaccharides induced brown discolouration accompanied by cellular breakdown (Yamaki et al., 1977). Chun et al. (2003) reported differences in the occurrence of this disorder among varieties and the close relationship of this phenomenon to the amount and composition of pectin-like substances. These findings suggest that

* Corresponding author.
E-mail addresses: nfukuoka@ishikawa-pu.ac.jp (N. Fukuoka), hamada@ishikawa-pu.ac.jp (T. Hamada), eishin@pref.ishikawa.lg.jp (E. Takeshita).
[1] NF and MM equally contributed to this paper.

https://doi.org/10.1016/j.plaphy.2018.12.007
Received 1 November 2018; Received in revised form 11 December 2018; Accepted 12 December 2018
Available online 15 December 2018

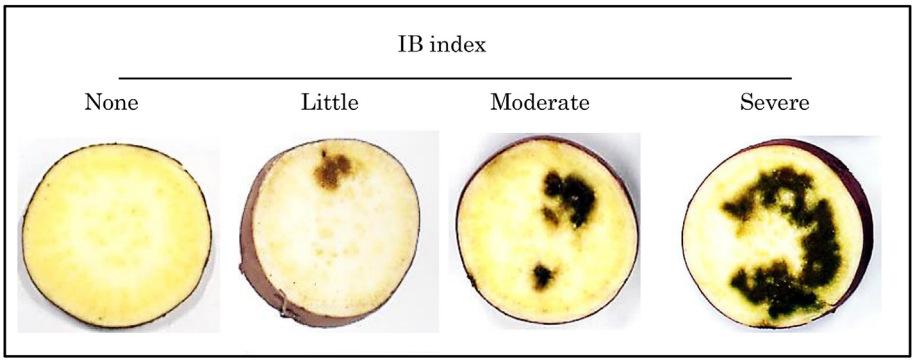

Fig. 1. Images of representative tissues of IB disorder classified in this study. The severity was classified into five levels based on the ratio of browned to total tissue (*rbt*): none (IB index 0), slight (IB index 1; approx. $rbt < 5\%$), little (IB index 2; approx. $5\% \leq rbt < 10\%$), moderate (IB index 3; approx. $10\% \leq rbt < 30\%$), and severe (IB index 4; approx. $rbt \geq 30\%$) discoloration.

intervarietal differences in IB disorder in sweetpotato may be due to interactions among the accumulation of starch grains, the amount and composition of pectin-like substances in the cell wall, ROS generation, and polyphenol biosynthesis, among other physiological factors.

The aim of the present study was to clarify the mechanism of IB occurrence in sweetpotato. To accomplish this objective, IB-susceptible cv. Goroujima-Kintoki and IB-resistant cv. Koukei 14 were selected, and the morphology of starch grains, the amount and composition of pectin-like substances on the cell wall, ROS generation, and polyphenol biosynthesis were compared. In this paper, we suggest that IB occurrence of sweetpotato is largely dependent on the difference in the extent of decomposition of highly pectic polysaccharides on the cell wall linked with differences in intracellular ROS generation resulting from the morphology and accumulation timing of starch grains during root maturation period.

2. Materials and methods

2.1. Plant materials

Two cultivars of sweetpotato, Goroujima-Kintoki (hereafter, “Goroujima”) and Koukei 14 (hereafter, “Koukei”), were grown in sandy loam soil at the experimental farm of Ishikawa Sand Dune Agricultural Research Center, located in Kahoku City of Ishikawa Prefecture in Japan. Vine cuttings (ca. 30 cm) of each cv. were taken from plant nursery beds and transplanted on 20 May 2015 and 2016 in 4 rows 12 m long that were spaced 0.8 m apart. In both years, spacing between plants within rows was 0.4 m, giving a sweetpotato population of 3120 plants per 10 a. A basal fertiliser of 16.5 g m^{-2} N, 22.0 g m^{-2} P_2O_5, and 31.9 g m^{-2} K_2O was applied before ridge plowing.

To examine the correlation between the occurrence of IB and its related physiological characteristic, 14 plants from each variety were sampled at 90, 120, and 150 days after planting (DAP) in both years, and ten uniform plants were selected for determination of IB disorder occurrence. All harvested roots with a weight of 50 g or more were cut transversely at 1 cm intervals. Then, the disks with the most severe symptoms were selected and used to classify the level of IB disorder for that plant at each time point based on qualitative and quantitative appearance as the ratio of browned to total tissue (*rbt*) as follows: none (IB index 0), little (IB index 1, approx. $rbt < 10\%$), moderate (IB index 2; approx. $10\% \leq rbt < 30\%$), and severe (IB index 3; approx. $rbt \geq 30\%$)(Fig. 1).

Then, anatomical and histochemical studies as well as quantification of metabolic products were conducted on the midportion of 120-day-old roots collected in 2015. For the anatomical study, three disks, each with a thickness of about 1 cm, were taken from roots categorised as IB index 0. Cubes (about 1 cm on each face) were collected from about 1 to 2 cm inside the epidermis using a sharp paring knife. Each cube was fixed in FAA [50% (v/v) ethanol, 10% (v/v) formaldehyde, and 5% (v/v) acetic acid] at room temperature and stored in the solution. For histochemical observations, cubes from normal and affected regions in cv. Goroujima with IB index 1 and from normal region in cv. Koukei with IB index 0 were collected from about 1 to 2 cm inside the epidermis of the disks. Since the degree of IB disorder in cv. Koukei was minimal and rarely occurred, the material required for histochemical observations could not be secured. For the same reason, measurement of metabolic products was also conducted using the disks categorised into IB index 0 and/or 1. After removing approximately 1 cm around the edge of disk, the tissues from normal and affected regions in cv. Goroujima with IB index 1 and from normal region in cv. Koukei with IB index 0 were shredded with a sharp paring knife and stored at −45 °C until analysis. Pectin substances and expression of genes related to starch and polyphenol biosynthesis were measured using disks from the midportion of 120- and 150-day-old roots categorised into IB index 0 in 2016. The analytical materials were prepared in the same way as shown in the measurement of metabolic products and stored at −45 °C.

2.2. Anatomical observation

Fixed tissues were dehydrated using a graded ethanol series [3 h at each of 40%, 60%, 70%, 85%, 95% and 100% (v/v) ethanol], embedded in paraffin (Ikeshita et al., 2010), and cut transversely into 15 μm sections using a PR-50 microtome (Yamato Kohki Inc., Saitama, Japan). The sections were placed on silane-coated glass slides, incubated overnight on a hot plate at 50 °C and deparaffinised according to manufacturer instructions. Parenchyma cells around secondary vascular tissue were observed under a biological light microscope (MT5300 L; Meiji Techno Co. Ltd., Saitama, Japan). Images were digitised by EOS Utility software (Canon Inc., Tokyo, Japan), and the number of starch grains per cell and the length of starch grains were measured using NIH Image software (http://rsb/info.nih.gov/nih-image).

2.3. Histochemical observation

Cubes (about 1 cm × 1 cm × 1 cm) cut from normal and affected regions, from about 1 to 2 cm inside the epidermis were excised, immediately sliced at approximately 100 μm intervals using a microslicer (DTK-1000; Dosaka EM, Kyoto, Japan) and soaked in distilled water.

For histochemical detection of polyphenol oxidase (PPO), sections were mounted in McIlvaine buffer (pH 5.0) containing 20 mM 4-chlorocatechol, held in the dark at room temperature for 5 min and observed under a biological light microscope (MT5300 L). In this reaction, brown precipitate indicates the presence of PPO. Histochemical localisation of chlorogenic acid was performed according to the method of Rhee and Iwata (1982). The sections were mounted on slides with the addition of a few drops of ammonia solution (28% w/w). Immediately thereafter, yellow precipitate was imaged under a light microscope (MT5300 L). Hydrogen peroxide was visually detected using 3, 3-diaminobenzidine (DAB) (Sigma-Aldrich, St. Louis, MO, USA) as substrate following the method described by Orozco-Cárdenas and Ryan (1999). The section was placed on a slide containing DAB solution (1 mg/ml,

pH 3.8) for 1 h in the dark at room temperature to allow the deep-brown polymerisation product (reaction of DAB with H_2O_2) to be visualised and thereafter was imaged under a light microscope (MT5300 L). The hydroxyl radical was detected using aminophenyl fluorescein (APF) dye-based kit (Cell Technology Inc., Mountain View, CA, USA). The section was placed on a slide containing 5 μM APF solution in phosphate buffer (0.1 M, pH 7.4) for 5 min in the dark at room temperature and thereafter, the fluorescence of the oxidised APF (excitation/emission: 490 nm/515 nm) was imaged under an AXIO Imager M1 microscope (Carl Zeiss, Oberkochen, Germany).

2.4. Starch content

Each frozen sample (5 g) was added to 20 ml of 80% (v/v) ethanol in a polypropylene tube and homogenised for 2 min. The tubes equipped with glass cooling pipes were transferred to an 80 °C water bath, and after incubation for 2 h, the tubes were centrifuged at 10,000 rpm for 10 min, and the supernatant was discarded. The sediment was extracted twice more in the same way, and 10 ml of 80% (v/v) ethanol was added to the residue and allowed to stand at room temperature overnight. Then, the tubes were centrifuged at 10,000 rpm for 10 min and the supernatant was discarded. The residues were hydrolyzed with 30 ml of 0.5 N HCl in a boiling water bath for 2 h, and the hydrolysate was neutralised with about 3 ml of 5 N NaOH. After removing the precipitate by filtration through filter paper (Advantec Toyo No. 2; Toyo Roshi, Tokyo, Japan), the supernatant was brought up to 100 ml with distilled water and then diluted 500-fold with distilled water. An aliquot (0.25 ml) of diluted solution was mixed with 0.25 ml of 5% phenol solution, and 1.25 ml of concentrated sulphuric acid was subsequently added. Then, the mixture was shaken, and the starch content was measured as the absorbance at 490 nm using a U-3900 spectrophotometer (Hitachi Co. Ltd., Tokyo, Japan) and compared to a standard curve based on glucose. Total starch content was expressed as grams of glucose per 100 g fresh weight of root.

2.5. Enzyme assays

To determine peroxidase (POD) activity, 0.25 g of each frozen sample was homogenised in 25 ml of 50 mM phosphate buffer (pH 6.5). In a reaction mixture (2.5 ml) consisting of 25 μl of crude extract, 0.25 ml 50 mM phosphate buffer (pH 6.5), 50 μl 0.15% (v/v) H_2O_2, and 0.25 ml 10 mM pyrogallol, POD activity was determined at 430 nm using a U-3900 spectrophotometer (Hitachi Co. Ltd., Tokyo, Japan) and was expressed as purpurogallin formed per milligram fresh weight of root per minute.

PPO activity was assayed according to the method of Koukol and Conn (1961) with some modifications. Approximately 1.0 g of each frozen sample was added to 0.25 g PVPP and homogenised in 25 ml of 50 mM phosphate buffer (pH 7.0). The homogenate was centrifuged at 10,000 rpm at 4 °C for 10 min, and the supernatant was used as a crude enzyme extract. The reaction mixture consisted of 1.0 ml of 50 mM HEPES buffer (pH 7.5), 1.0 ml 1% (w/v) catechol and 0.1 ml of crude extract. PPO activity was determined at 420 nm and was expressed as quinone derivatives formed per milligram fresh weight of root per minute.

2.6. Polyphenol content

Each 5 g frozen sample (n = 3–4) was homogenised in 20 ml of 80% (v/v) methanol and allowed to stand undisturbed overnight at 4 °C. The methanolic extract was centrifuged at 10,000 rpm at 4 °C for 10 min, and the supernatant was used as the extract solution. Total phenol content was measured using the method described by http://www.sciencedirect.com/science/article/pii/S0023643807003829, Singleton et al. (1999) with some modifications. A 10 μl aliquot of solution was brought up to 40 μl with distilled water in each well of a 96-well microplate. Then, 50 μl of Folin-Ciocalteau reagent and 50 μl of 100 mg/l Na_2CO_3 were added to each well. After incubation for 60 min at room temperature, the absorbance at 750 nm was measured using a plate reader (Bio-Rad, Hercules, CA, USA). Results were expressed as milligrams of gallic acid equivalent per 100 g fresh weight of root.

2.7. H_2O_2 content

To determine H_2O_2 content, 0.5 g of each frozen sample was homogenised in 25 ml 100 mM phosphate buffer (pH 6.5). A 50 μl aliquot of each solution was transferred to a 96-well microplate. A working solution of the Amplex Red Hydrogen Peroxide Assay Kit (Molecular Probes Inc., Eugene, OR, USA) was then freshly prepared following the manufacturer's protocol, and 50 μl was added to each well. The mixtures were placed in the dark for 30 min at room temperature and the absorbance was measured at 576 nm using a U-3900 spectrophotometer (Hitachi Co. Ltd., Tokyo, Japan).

2.8. Gene expression related to sugar and polyphenol biosynthetic pathway

We extracted RNA using a modified version of the CTAB method (Kim and Hamada, 2005). Approximately 1 g of frozen samples was pulverised using a mortar and pestle in the presence of liquid nitrogen. The frozen powder was mixed thoroughly with 10 ml extraction buffer (2% CTAB, 1.0 M NaCl, 10 mM Tris-HCl, pH 9.5 and 5 mM EDTA). The samples were mixed with an equal volume of chloroform:isoamyl alcohol (24:1, v/v) by inversion for 15 min and then centrifuged at 15,000 rpm for 10 min at 4 °C. Each supernatant was taken up and mixed with 0.25 vol of 10 M LiCl, and then held at −20 °C for 4 h. Total RNAs were precipitated by centrifugation at 15,000 rpm for 10 min at 4 °C. The supernatant was removed, and RNA pellets were washed twice with 1 ml 70% (v/v) ethanol. The pellets were dried for 10 min at 37 °C and dissolved in 500 μl TE buffer.

Aliquots of total RNA (200 ng) were reverse-transcribed to cDNA using a ReverTra Ace qPCR RT Master Mix with gDNA Remover (Toyobo, Osaka, Japan) as follows: samples were denatured at 65 °C for 5 min and placed on ice, then DNase treatment was conducted by adding 2 μl 4 x DN Master Mix with gDNA remover in an 8 μl reaction and incubating at 37 °C for 5 min, followed by reverse transcription in a 10 μl reaction containing 2 μl 5 × DN Master Mix at 37 °C for 15 min and at 50 °C for 5 min and termination at 98 °C for 5 min. The obtained cDNA samples were stored at −20 °C until use.

The relative content of mRNA was determined on 1:10 dilution of cDNA by real-time polymerase chain reaction (PCR) on a StepOnePlus system (Applied Biosystems, Foster City, CA) using the primers for each of the following nine genes related to sugar and polyphenol metabolism: sucrose synthase (*IbSuSy*), acid invertase (*IbAINV*), neutral invertase (*IbNINV*), granule bound starch synthase (*IbGBSS*), starch branching enzyme 1 (*IbSBE1*), starch branching enzyme 2 (*IbSBE2*), glucose-6-phosphate dehydrogenase (*IbG6PD*), phenylalanine ammonia-lyase (*IbPAL*) and polyphenol oxidase (*IbPPO1*) (Table 1). Each 20 μl mixture contained 1 μl cDNA, 0.4 μl of each primer (10 pmol/μl), 0.2 μl 100 × CXR, 8 μl nuclease-free water, and 10 μl qPCR Master mix (Promega Corp., Madison, WI, USA). The PCR conditions were as follows: 95 °C for 2 min for the initial denaturation step, followed by 40 cycles of 95 °C for 15 s and 60 °C for 1 min. The transcript levels of each gene were normalised to that of the tubulin gene as a control. Relative gene expression was determined by the ΔΔCT method. All measurements were made in triplicate and the mean values were calculated.

2.9. Pectin substances

Alcohol insoluble solids (AIS) were prepared according to the method of Swingle (1966) with some modification. For AIS constituent analyses, approximately 8–10 g of frozen samples was blended with

Table 1
Primers for quantitative reverse transcription–polymerase chain reaction analysis.

Gene	Gene bank accession no.	Forward Primer (5′→3′)	Reverse Primer (5′→3′)
IbSuSy	CA409457	GCCACGTGTACTTCTCCTGGAT	CCTTCCCACTGGGAAACCAT
IbAINV	AB775770	CCACCTACCATTCGCCATGG	GCAAGACCCCATCCAAGAGC
IbNINV	AB125887	TCCAGTTCGTAAGACTGATGCAA	CACAGGAGCGACTCTTCCAAT
IbGBSS	AB071976	CCAGCAAAAATGGAAGGGAAA	TTCATCCCTTGTTGTTTACACACA
IbSBE1	AB194725	TGGCCAATACTCTGATCCACAGT	CAGGCATACCAGACACATCTTCA
IbSBE2	AB042937	CGAATTTCTTTGCACCAAGCA	CATGGGCTCTATCAATCAAAGATTT
IbG6PD	BM878844	CGCGGAGTGTGATAAGTTGTGT	TCAGTTTCTTCGCTGTAGTTTCCTT
IbPAL	M29232	TGTATCA AGAAGCAGCAGGTTGAT	GTGGCTCCCCCTCAATGAC
IbPPO1	AB038994	C CCAAAACCCTCTCAGATCCA	TTGCATGAGACCTTGAAATGGT
Tubulin	AB572296	CAGAGGGCTGTTGCATGATC	CAAACTTATGGTCAATGCGAGAGA

Table 2
Intervarietal differences in the occurrence of IB.

Year	Cultivar	DAP	Roots with IB (%)			
			None	Little	Moderate	Sever
2015	Goroujima	90	100.0	0.0	0.0	0.0
		120	98.1	1.9	0.0	0.0
		150	82.0	16.0	0.0	2.0
	Koukei	90	100.0	0.0	0.0	0.0
		120	95.2	4.8	0.0	0.0
		150	98.0	2.0	0.0	0.0
2016	Goroujima	90	92.9	7.1	0.0	0.0
		120	81.8	18.2	0.0	0.0
		150	85.5	5.8	2.9	5.8
	Koukei	90	100.0	0.0	0.0	0.0
		120	100.0	0.0	0.0	0.0
		150	98.6	1.4	0.0	0.0

The severity of IB symptoms was classified into the following four levels based on the ratio of browned to total tissue browning (*rbt*); none (IB index 0), little (IB index 1; approx. $rbt < 10\%$), moderate (IB index 2; approx. $10\% \leqq rbt < 30\%$), and severe (IB index 3 approx. $rbt \geq 30\%$) discoloration.

30 ml of 90% (v/v) ethanol in test tubes and homogenised for 2 min. The test tubes equipped with glass cooling pipes were transferred to an 80 °C water bath and incubated for 3 h followed by centrifugation at 10,000 rpm for 10 min after which the supernatant was discarded. The sediment was washed three times in the same way. The precipitate was allowed to air dry at room temperature overnight and then ground using a mortar and pestle. Subsequently, the ground AIS residue was oven dried overnight and used for pectin determinations.

A 0.3–0.5 g aliquot of AIS residue was mixed with 100 ml of 0.5% (w/v) ammonium oxalate, and the mixture was stirred with a magnetic stirrer for 3 h. The suspension was filtered with the aid of suction through Whatman No. 1 filter paper (GE Healthcare, Chicago, IL, USA) on a Buchner funnel connected to a vacuum pump. The traced filter paper and its container were then dried at 100 °C overnight, and the weight of residue was estimated as soluble pectin (fraction A).

To determine the protopectin content, a 0.3–0.5 g aliquot of AIS was mixed with 50 ml of 0.5% (w/v) ethylenediaminetetraacetic acid tetrasodium salt (pH 11.5), and the mixture was stirred for 30 min at room temperature. The pH was then reduced to 5.5 by the addition of reagent acetic acid. The suspension was added to 10 ml of 1% pectinase (Tokyo Chemical Industry Co., Ltd., Tokyo, Japan) and stirred for 2 h at 35 °C. The residue was dried after filtration, and the weight of the residue was referred to as fraction B. The weight loss calculated as fraction B minus fraction A was estimated as the protopectin content.

3. Results

3.1. Incidence of IB

Differences in the incidence of IB formation were clearly observed between the two cultivars (Table 2) with the root of cv. Goroujima being more susceptible to IB disorder than that of cv. Koukei. In 2015, 16% of cv. Goroujima roots exhibited IB index 1 (little) at 150 DAP compared to only 2.0% of for cv. Koukei. The severity of IB generally increases with age, with intensity in cv. Goroujima progressively increasing in 2016 to a total of 8.7% of roots showing moderate or severe IB at 150 DAP. On the other hand, in cv. Koukei, only 1.4% of roots exhibited IB at the level of “little” even at 150 DAP.

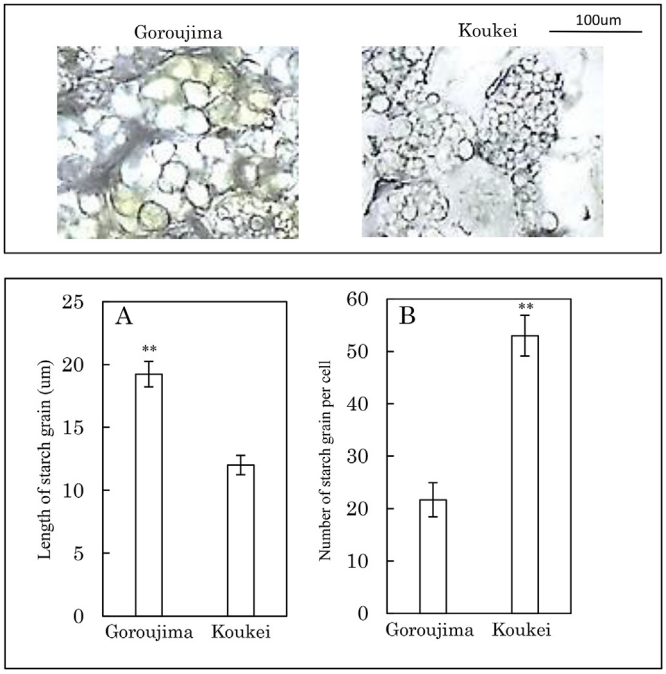

Fig. 2. Differences in morphology of starch grains in cells around secondary vascular tissue in the tuberous root. Anatomical study was conducted on the midportion of 120-day-old roots collected in 2015. Cubes (about 1 cm on each face) were collected from about 1 to 2 cm inside the epidermis from roots categorised as IB index 0. Upper panel; state of starch grain in cells, Lower panel A; mean length of starch grain, Lower panel B; number of starch grains per cell. Error bars indicate SE (n = 6–7). ** indicates statistically significant differences at $p < 0.01$ by the Mann-Whitney *U* test.

3.2. Status of starch grains in cells around secondary vascular tissue

Although cells around the secondary vascular tissue were filled with starch grains in both cultivars, the size of accumulated starch grain in cell differed between the two cultivars (Fig. 2 upper panel). Cells in cv. Gorojima consisted of large starch grains and the number of them was small, whereas many small starch grains accumulated in cells in cv. Koukei. The mean length of starch grains in cells of cv. Goroujima (approx. 20 μm) was 1.6 times larger than that in cv. Koukei (Fig. 2

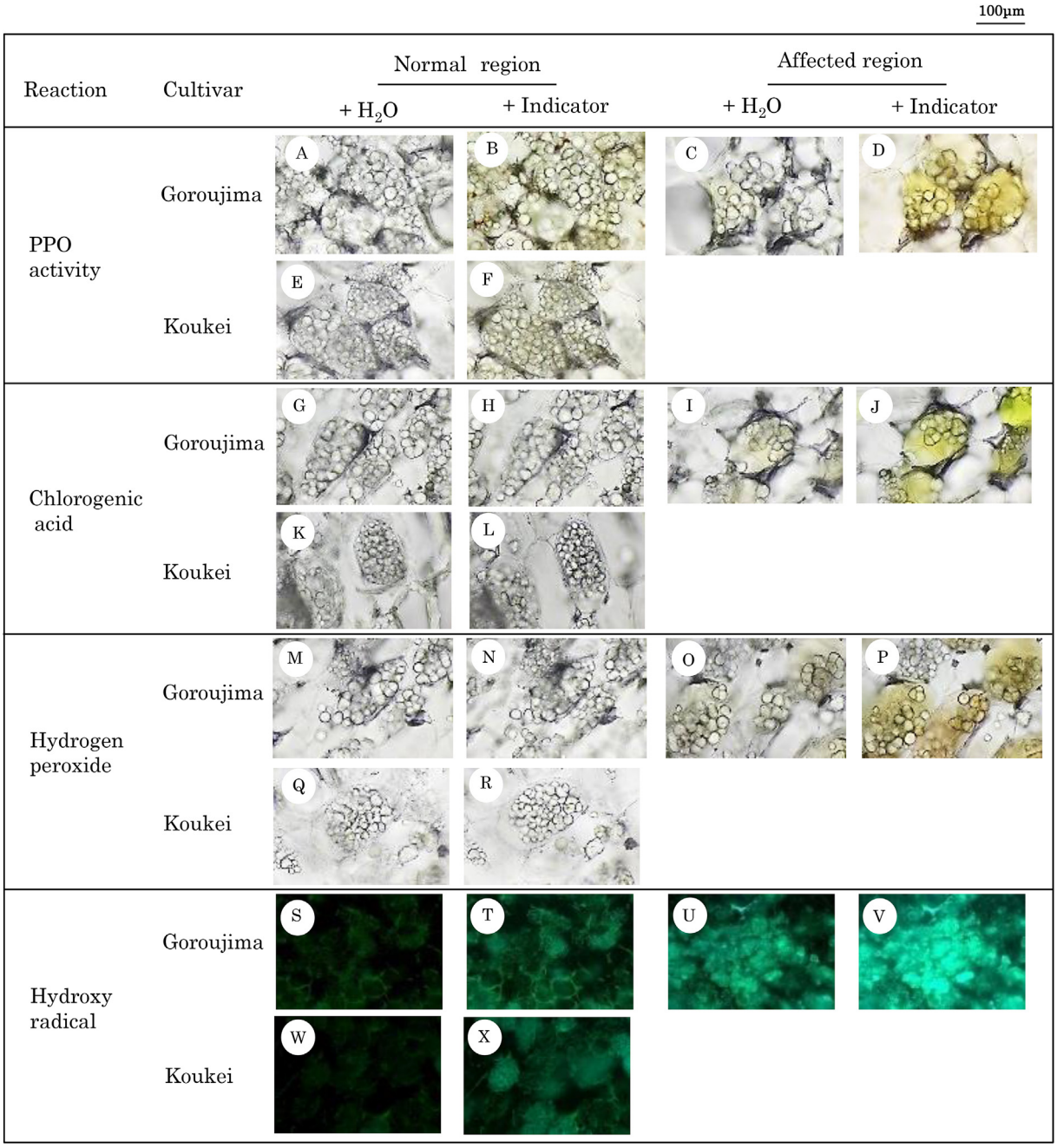

Fig. 3. Histochemical observation of PPO activity (A–F), chlorogenic acid (G–L), hydrogen peroxide (M–R), and hydroxy radical (S–X) at the parenchyma cells around secondary vascular tissue. Histochemical observations were conducted on the midportion of 120-day-old roots collected in 2015 and performed on cells around secondary vascular tissues from normal and affected regions in cv. Goroujima with IB index 1 and from normal region in cv. Koukei with IB index 0. Successive transverse sections were stained in the absence (A, C, E, G, I, K, M, O, Q, S, U, W) or presence (B, D, F, H, J, L, N, P, R, T, V, X) of indicator.

lower panel A), while the number of starch grains per cell in cv. Koukei was 2.5 times larger (Fig. 2 lower panel B).

3.3. Histochemical observation of cells around secondary vascular tissue

Cells around the secondary vascular tissues were observed in samples from normal and affected regions in cv. Goroujima with IB index 1 and from normal region in cv. Koukei with IB index 0. In the normal region, chlorogenic acid and H_2O_2 were not observed in both cultivars (Fig. 3H, L, N, R), although there was a weak reaction of PPO activity in this region (Fig. 3B, F). On the other hand, strong reactions indicate the high presence of PPO activity, chlorogenic acid, and H_2O_2 in cells from affected regions in cv. Goroujima, producing an accumulation of yellow/brown precipitates (Fig. 3D, J, P). The fluorescence reaction of hydroxyl radical was similar to that of PPO activity; a stronger reaction was observed in cells from the affected region in cv. Goroujima compared to those from the normal regions in both cultivars (Fig. 3T, V, X).

3.4. Metabolic products

Starch content tended to be high in the affected region of cv. Goroujima compared to the normal regions of both cultivars, although these differences were not statistically different (Fig. 4A). On the other hand, significantly higher POD and PPO activities and polyphenol and H_2O_2 levels were detected in the affected region of cv. Goroujima compared to the normal regions of both cultivars (Fig. 4B, C, D, E). POD

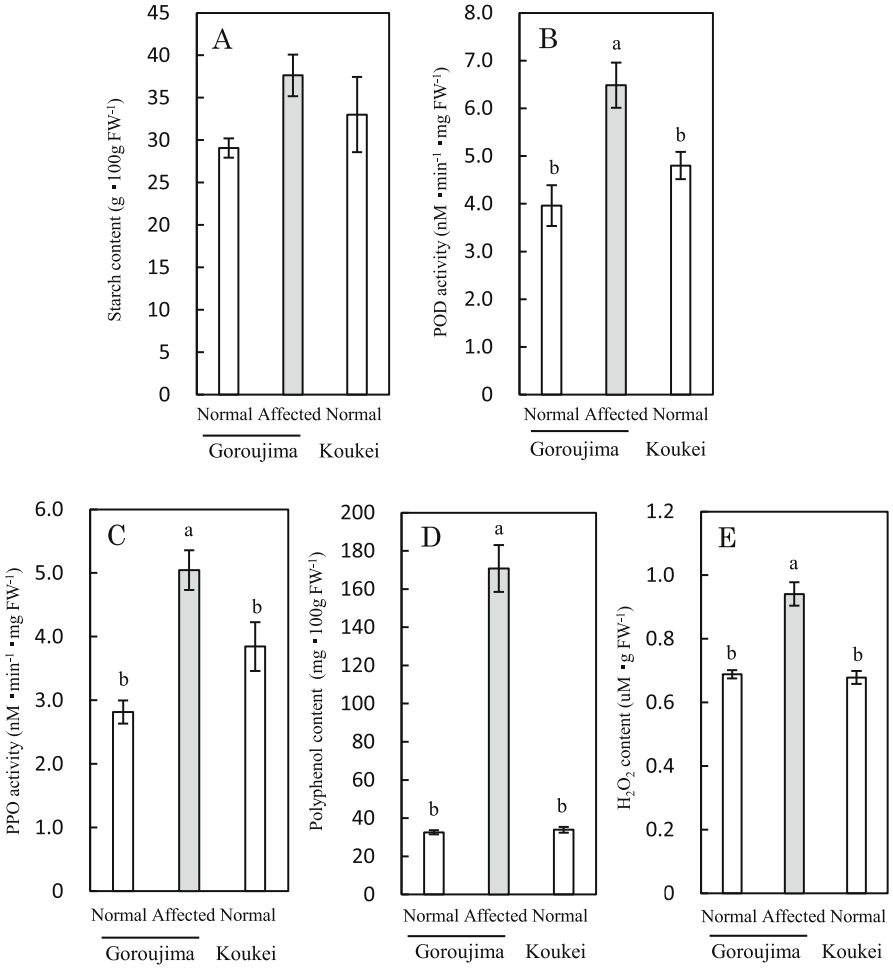

Fig. 4. Differences in starch contents (A), POD activity (B), H_2O_2 content (C), PPO activity (D), and polyphenol content (E) in tuberous root. The measurement of metabolic products was conducted on the midportion of 120-day-old roots collected in 2015 using tissues from normal and affected regions in cv. Goroujima with IB index 1 and from normal region in cv. Koukei with IB index 0. Error bars indicate ± SE (n = 4–5). Different letters indicate significant differences at the 5% level by Tukey's multiple range test.

and PPO activities were elevated by 135%–164% and 131%–179%, respectively, in the affected region of cv. Goroujima compared to normal regions of both cultivars. Polyphenol and H_2O_2 levels were 503%–527% and 137%–139%, respectively, higher in the affected region of cv. Goroujima compared to normal regions of both cultivars.

3.5. Gene expression related to sugar and polyphenol biosynthesis

Expression levels of genes were measured using disks of 120- and 150-day-old tuberous roots categorised as IB index 0. The transcriptional levels of all genes in cv. Goroujima were higher in the early stage (120 DAP) than late stage (150 DAP). Conversely, in cv. Koukei, the levels were lower than those in cv. Goroujima in the early stage (120 DAP), and increased or remained almost the same in the late stage (150 DAP). At 120 DAP, the levels of genes related to sugar biosynthesis (*IbSuSy*, *IbAINV*, *IbNINV*) in cv. Goroujima were approximately 190%–530% of the values in cv. Koukei (Fig. 5A, B, C), Likewise, at 120 DAP, genes related to starch biosynthesis (*IbGBSS*, *IbSBE1*, *IbSBE2*) were approximately 330%–380% higher (Fig. 5D, E, F) and those for polyphenol (*IbG6DG*, *IbPAL*, *IbPPO*) biosynthesis were 160%–420% higher (Fig. 5G, H, I).

3.6. Pectin substances

Although the levels of pectin-like substances in roots between cultivars were not statistically different (Fig. 6), the concentration of protopectin in cv. Goroujima tended to be lower than that in cv. Koukei at 150 DAP. The protopectin content in cv. Goroujima at 150 DAP was 0.016 g/g FW, which was approximately 60% of the values in cv. Koukei (Fig. 6B).

4. Discussion

In this study, differences in IB formation were clearly observed between the cultivars (Table 2). Root of cv. Goroujima was susceptible to IB disorder, whereas the cv. Koukei tested here was resistant to IB. Our previous report (Fukuoka et al., 2018) revealed that IB damage initially occurs in the cells around the secondary vascular tissue, and the area per cell occupied by starch grains in this region was larger than in the unaffected region. Thus, we examined the intervarietal differences related to the morphology of starch grains in cells around secondary vascular tissue in this study (Fig. 2). Anatomical observations revealed that cells around the secondary vascular tissue were filled with starch grains for both cultivars but the size of accumulated starch grains in cells differed between the two cultivars. Cells in cv. Gorojima consisted of large starch grains and the number of them was small, whereas many small starch grains accumulated in cells in cv. Koukei. This result suggests that not only the degree of saturation of the starch grains within the cell, but also the size of the accumulated starch grains are closely related to the occurrence of IB disorder. We hypothesize that IB

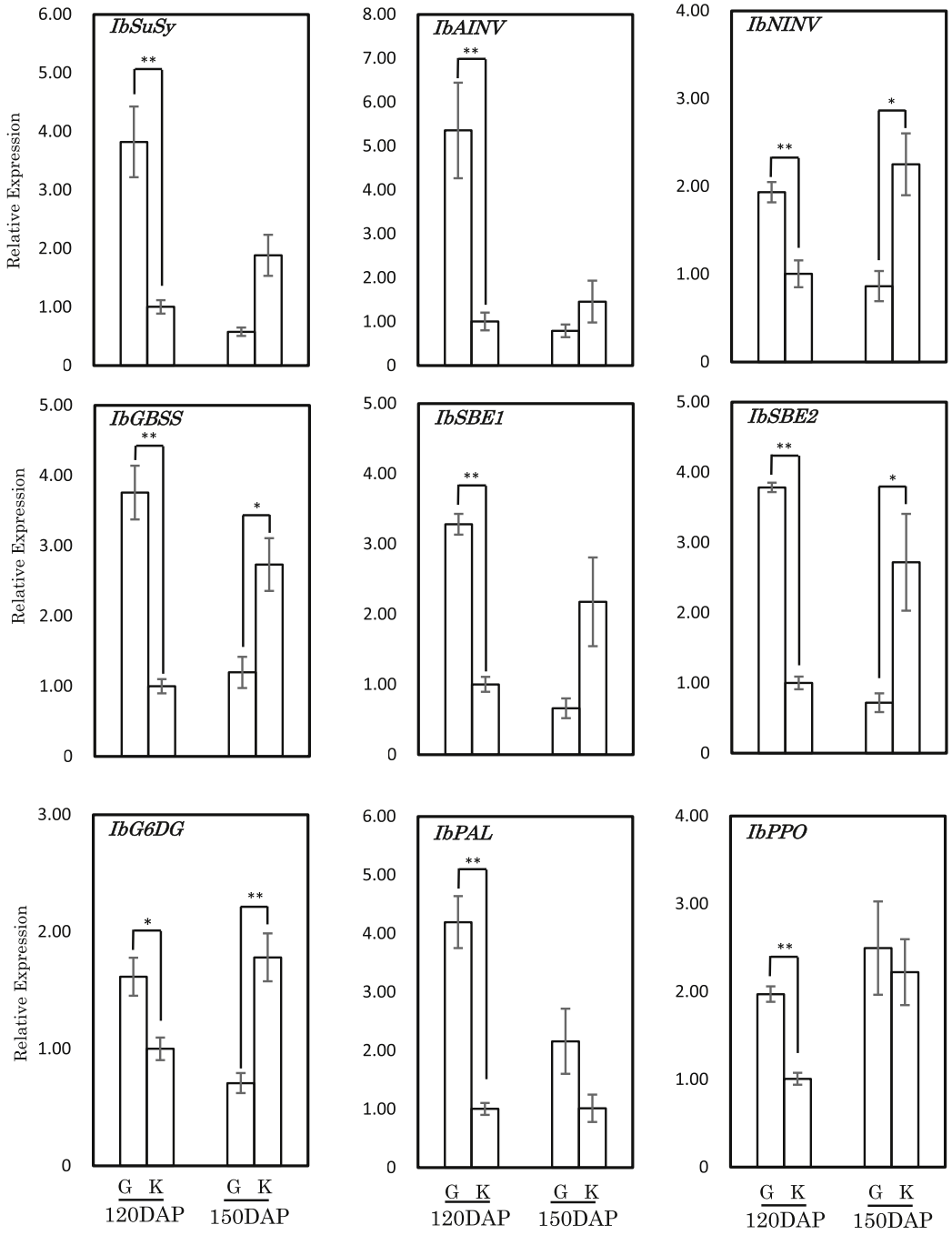

Fig. 5. Differences in expression of genes in the tuberous root during maturation. K; Koukei, G; Goroujima. Expression of genes related to starch and polyphenol biosynthesis was measured using disks from the midportion of 120- and 150-day-old roots categorised into IB index 0 in 2016. Error bars indicate SE (n = 3–4). * and ** indicate statistically significant differences at $p < 0.05$ and $p < 0.01$, respectively, by the Mann-Whitney U test.

disorder is likely to occur in cells around the secondary vascular tissue in which large starch grains accumulate excessively.

Generally, accumulation of ROS in tissues accelerates the disruption of metabolic function and loss of cellular integrity (Foyer et al., 1991). Membrane deterioration caused by ROS is thought to be related to peroxidation of membrane lipids (Panavas and Rubinstein, 1998; Dhindsa et al., 1981) and decomposition of pectin (Inari and Takeuchi, 2001). PPO, known as catechol oxidase, contributes to the development of tissue browning by oxidizing accumulated phenolics into quinones (Hyodo et al., 1978). PPO is localized in an inactive form in the chloroplast, where it is bound to thylakoid membranes (Vaughn and Duke, 1981, 1984), and its activity is initiated by the disruption of cellular integrity (Chikezie et al., 2013). Thus, we histochemically examined the accumulation of polyphenols, ROS, and related enzymes in cells from normal and affected regions in cv. Goroujima and from normal region in cv. Koukei (Fig. 3). The results revealed strong reactivity indicative of ROS generation and polyphenol biosynthesis in cells from affected regions in IB-susceptible cv. Goroujima. Of note, these types of active responses were never observed in IB-resistant cv. Koukei, which has small starch grain size (Fig. 2). These results suggest that excessive accumulation of large starch grains within the cells triggers ROS generation and subsequent biosynthesis of polyphenols. In our previous report (Fukuoka et al., 2018), we also showed that accumulation of large starch grains within the cells promotes ROS

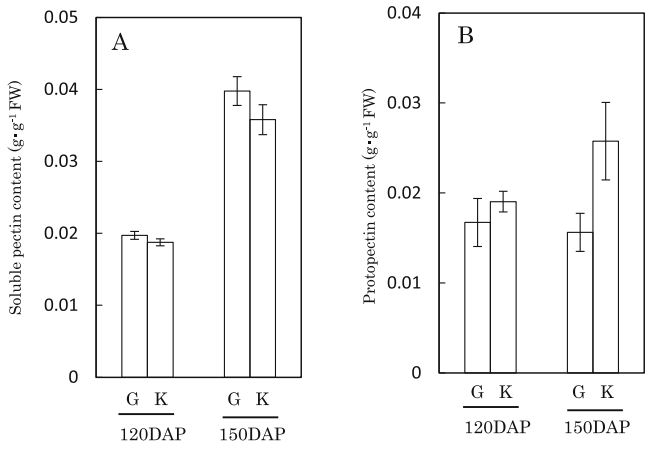

Fig. 6. Differences in the content of pectic substance in tuberous root during root maturation period. Pectin substances were measured using disks from the midportion of 120- and 150-day-old roots categorised into IB index 0 in 2016. A; soluble pectin content, B; protopectin content, G; Goroujima, K; Koukei. Error bars indicate SE (n = 3–4).

generation and that generation of ROS on a large scale leads to membrane deterioration, resulting in activation of polyphenol biosynthesis.

Here, it is not clear why the ROS generation was kept low in IB-resistant cv. Koukei even though cells had a large number of starch grains. Since ROS like H_2O_2 act as a signaling molecule mediating the acquisition of tolerance to both biotic and abiotic stresses (Bhattacharjee, 2005), abundant ROS generation within the cells in IB-susceptible cv. Goroujima may be caused by an increase in the turgor pressures of cells due to the excessive accumulation of starch grains with large size (Fig. 2). In contrast, since IB-resistant cv. Koukei is composed of small starch grains (Fig. 2), starch grains can adhere to each other making it unlikely that turgor pressure increases due to ROS generation. Further research is necessary to elucidate the correlation between patterns of starch accumulation and ROS generation within cells.

In addition to the histochemical observation of metabolic products, starch content, H_2O_2 concentration, POD activity, polyphenol content and PPO activity were also quantified in this study. Starch content tended to be higher in the affected region of cv. Goroujima compared to in normal regions of both cultivars (Fig. 4A). Higher POD activity and H_2O_2 content were clearly detected in the affected region of cv. Goroujima compared to in normal regions of both cultivars (Fig. 4B and E). PPO activity and polyphenol content over time showed a pattern identical to that of H_2O_2 content (Fig. 4C and D). These results support the above hypothesis that abundant ROS generation induced by accumulation of large starch grains within the cells leads to activation of polyphenol biosynthesis.

NINV in the cytosol cleaves sucrose into glucose and fructose. Apoplastic sucrose is also hydrolyzed to glucose and fructose by AINV followed by the uptake of monosaccharides by hexose transporters (Wind et al., 2010). SuSy reversibly catalyzes the conversion of sucrose into UDP-glucose and fructose in the cytosol (Li and Zhang, 2003). After conversion of UDP-glucose to glucose-1 P by pyrophosphorylase, AGPase catalyzes the conversion of glucose-1 P to ADP-glucose (Kim et al., 2002). The ADP-glucose formed in the cytosol is presumably transported into the plastids, and there, starch grains are synthesized by GBSS (Otani et al., 2007), SBE1 and SBE2 (Hamada et al., 2006; Shimada et al., 2006). Expression analysis of genes encoding enzymes involved in starch synthesis in this study showed that in IB-susceptible cv. Goroujima, transcription levels of all genes (*IbSuSy, IbAINV, IbNINV, IbGBSS, IbSEB1, IbSBE2*) peaked at an early stage of root maturation, and the levels decreased as roots matured (Fig. 5). Conversely, in cv. Koukei, the levels were low early and increased moderately to the later stage of root development (Fig. 5). These results strongly show that IB-susceptible cv. Goroujima actively begins starch synthesis from earlier stages of root maturation compared to IB-resistant cv. Koukei.

G6PDH is the rate-limiting enzyme of the pentose phosphate pathway, which produces precursors for phenolic secondary metabolite synthesis (Ali et al., 2006). PAL is the key enzyme in the phenylpropanoid pathway that is involved in the formation of cinnamic acid, coumarin, chlorogenic acid, etc. (Shen et al., 2006). PPO catalyzes the oxidation of phenolic compounds to quinones. In this study, in order to clarify whether biosynthesis of polyphenols is linked to starch biosynthesis, expression analysis of *IbG6HDH*, *IbPAL* and *IbPPO* was performed, and a pattern identical to the genes related to starch biosynthesis was demonstrated (Fig. 5). Transcription levels of all genes were higher at the earlier stage of root maturation in IB-susceptible cv. Goroujima, while the levels remained relatively lower at the early stage of root maturation in IB-resistant cv. Koukei. These facts strongly suggest that polyphenol biosynthesis is associated with active starch synthesis and that high starch accumulation from an early stage of root maturation triggers active polyphenol biosynthesis.

The concentration and composition of pectin-like substances in pear fruit are known to vary among cultivars (Chun et al., 2003), with higher ROS production during stress conditions enhancing fruit softening (https://www.sciencedirect.com/science/article/pii/S0925521415301150, Paliyath and Droillard, 1992) and causing a breakdown of insoluble protopectin into soluble pectin (Singh et al., 2018). According to Fukuoka and Enomoto (2014), intervarietal differences in the severity of IB disorder largely depend on the concentration or composition of pectin-like substances in radish roots. Furthermore, roots with high concentrations of protopectin are less prone to cell disruption induced by ROS toxicity. In this study, the composition and concentration of pectin-like substances in roots differed between the cultivars (Fig. 6). The concentration of protopectin in IB-resistant cv. Koukei tended to be higher than in susceptible cv. Goroujima. This observation suggests that intervarietal differences observed with regard to the severity of the IB disorder is largely associated with tolerance to the cell disruption caused by ROS being regulated by the concentration of protopectin. We think that cells in IB-resistant cultivars are hard to collapse because the concentration of protopectin remains high due to lower ROS generation. Conversely, cells in IB-susceptible cultivars were susceptible to disruption due to the depolymerisation of this cellular component resulting from higher ROS concentration. In pear fruit, the occurrence of watercore, which manifests as brown colouration accompanied by cellular breakdown (Yamaki et al., 1977), strongly intensifies as depolymerisation of pectic polysaccharides increases (Chun et al., 2003).

5. Conclusion

The occurrence of IB disorder in *I. batatas* largely depends on the morphology and timing of accumulated starch grain in cells around the secondary vascular tissues. IB-susceptible cultivars accumulate large starch grains within the cells from an earlier stage of root maturation. Abundant accumulation of large starch grains within the cells produces an increase in ROS concentration leading to the degradation of highly pectic polysaccharides in the cell wall. Thus, the cells finally collapse, and the increased PPO activity results in the accumulation of brown pigments. On the other hand, in resistant cultivars, membrane damage and the accompanying tissue browning was less likely to occur because ROS generation is kept low, owing to the accumulation of starch grains with small size.

CRediT authorship contribution statement

Nobuyuki Fukuoka: Conceptualization, Project administration, Supervision, Validation, Visualization, Writing – original draft. **Masahiro Miyata:** Investigation, Data curation, Formal analysis. **Tatsuro Hamada:** Writing – review & editing. **Eishin Takeshita:** Methodology.

References

Ali, M.B., Singh, N., Shohael, A.M., Hahn, E.J., Paek, K.Y., 2006. Phenolics metabolism and lignin synthesis in root suspension cultures of *Panax ginseng* in response to copper stress. Plant Sci. 171, 147–154.

Bhattacharjee, S., 2005. Reactive oxygen species and oxidative burst: roles in stress, senescence and signal transducation in plants. Curr. Sci. 89, 1113–1121.

Chikezie, P.C., Akuwudike, A.R., Chikezie, C.M., Ibegbulem, C.O., 2013. Fractional purification and kinetic parameters (K_m and V_{max}) of polyphenol oxidase extracted from three segments of *Solanum melongenas* and *Musa sapientum* fruits. Am. J. Plant Physiol. 8, 84–92.

Chun, J.P., Takamura, F., Tanabe, K., Itai, A., 2003. Physiological and chemical changes associated with watercore development induced by GA in Japanese pear 'Akibae' and 'Housui'. J. Jpn. Soc. Hortic. Sci. 72, 378–384.

Dhindsa, R.S., Plumbdhindsa, P., Thorpe, T.A., 1981. Leaf senescence: correlated with increased levels of membrane permeability and lipid peroxidation, and decreased levels of superoxide dismutase and catalase. J. Exp. Bot. 32, 93–101.

Foyer, C.H., Lelandais, M., Edwards, E.A., Mullineaux, P.M., 1991. The role of ascorbate in plants, interactions with photosynthesis, and regulatory significance. Curr. Top. Plant Physiol. 6, 131–144.

Fujita, E., Kouduma, M., Kajita, N., Kamimura, Y., Higashi, T., Torigoe, H., Yagami, S., Izumi, S., 2000. Improvement of internal brown spot of sweetpotato. Bull. Kagoshima Agri. Exp. Sta. 28, 13–21.

Fukuoka, N., Enomoto, T., 2001. The occurrence of internal browning induced by high soil temperature treatment and its physiological function in *Raphanus* root. Plant Sci. 161, 117–124.

Fukuoka, N., Enomoto, T., 2002. Enzyme activity changes in relation to internal browning of *Raphanus* root sown early and late. J. Hortic. Sci. Biotechnol. 77, 456–460.

Fukuoka, N., Enomoto, T., 2014. Relationship between the concentration of pectin-like substances and the severity of internal browning in radish (*Raphanus sativus* L.) roots induced by high soil temperature. J. Hortic. Sci. Biotechnol. 89, 625–630.

Fukuoka, N., Masuda, D., Ikeshita, Y., Kanamori, Y., 2009. Relationship between the occurrence of internal browning and anatomical and chemical factors in the tuberous root of sweet potato (*Ipomoea batatas* L.) cv. Kokei No. 14. Hortic. Res. (Japan) 8, 47–53.

Fukuoka, N., Miyata, M., Hamada, T., Takeshita, E., 2018. Histochemical observations and gene expression changes related to internal browning in tuberous roots of sweet potato (*Ipomea batatas*). Plant Sci. 274, 476–484.

Hamada, T., Kim, S.H., Shimada, T., 2006. Starch-branching enzyme I gene (*IbSBEI*) from sweet potato (*Ipomoea batatas*); molecular cloning and expression analysis. Biotechnol. Lett. 28, 1255–1261.

Hyodo, H., Kuroda, H., Yang, S.F., 1978. Induction of phenylalanine ammonia-lyase and increase in phenolics in lettuce leaves in relation to the development of russet spotting caused by ethylene. Plant Physiol. 62, 31–35.

Ikeshita, Y., Kanamori, Y., Fukuoka, N., Matsumoto, J., Kano, Y., 2010. Early cell enlargement by night-time heating of fruit produce watermelon fruit (*Citrullus lanatus Matsum*. et Nakai) with high sucrose content. Sci. Hortic. 126, 8–12.

Inari, T., Takeuchi, T., 2001. The effect of active oxygen on pectin. Bull. Gifu Women's Univ. 30, 1–7.

Kim, S.H., Hamada, T., 2005. Rapid and reliable method of extracting DNA and RNA from sweetpotato, *Ipomoea batatas* (L). Lam. Biotechnol. Lett. 27, 1841–1845.

Kim, S.H., Mizuno, K., Sawada, S., Fujimura, T., 2002. Regulation of tuber formation and ADP-glucose pyrophosphorylase (AGPase) in sweetpotato (*Ipomoea batatas* (L.) Lam.) by nitrate. Plant Growth Regul. 37, 207–213.

Kouklo, J., Conn, E.,E., 1961. The metabolism of aromatic compounds in higher plants. IV Purification and properties of the phenylalanine deaminase of *Hordeam vulgaare*. J. Biol. Chem. 236, 2692–2698.

Li, X.Q., Zhang, D., 2003. Gene expression activity and pathway selection for sucrose metabolism in developing storage root of sweet potato. Plant Cell Physiol. 44, 630–636.

Orozco-Cárdenas, M., Ryan, C.A., 1999. Hydrogen peroxide is generated systemically in plant leaves by wounding and systemin via the octadecanoid pathway. Proc. Natl. Acad. Sci. U. S. A 96, 6553–6557.

Otani, M., Hamada, T., Kim, S.H., Shimada, T., 2007. Inhibition of the gene expression for granule-bound starch synthase I by RNA interference in sweet potato plants. Plant Cell Rep. 26, 1801–1807.

Paliyath, G., Droillard, M.J., 1992. The mechanisms of membrane deterioration and disassembly during senescence. Plant Physiol. Biochem. 30, 789–812.

Panavas, T., Rubinstein, B., 1998. Oxidative events during programmed cell death of daylily (*Hemerocallis hybrid*) petals. Plant Sci. 133, 125–138.

Rhee, J.K., Iwata, M., 1982. Histological observations on the chilling injury of eggplant fruit during cold storage. J. Jpn. Soc. Hortic. Sci. 51, 237–243.

Shen, Q., Kong, F., Wang, Q., 2006. Effect of modified atmosphere packaging on the browning and lignification of bamboo shoots. J. Food Eng. 77, 348–354.

Shimada, T., Otani, T., Hamada, T., Kim, S.H., 2006. Increase of amylose content of sweetpotato starch by RNA interference of the starch branching enzyme II gene (*IbSBEII*). Plant Biotechnol. 23, 85–90.

Singh, N., Misra, K.K., Dongariyal, A., Rani, A., Nirgude, V., 2018. Response of different coating material on post-harvest life and quality of guava (*Psidium guajava* L.). Int. Chem. Stud. 6, 2635–2639.

Singleton, V.L., Oethofer, R., Lamuela-Raventos, R.M., 1999. Analysis of total phenols and other oxidation substrates and antioxidants by means of Folin-Ciocalteu reagent. Methods Enzymol. 299, 152–278.

Swingle, H.D., 1966. The Relation of Pectic Substances and Starch to Consistency and Moistness of Sweet Potatoes. LSU Historical Dissertations and Theses 1173. .

Vaughn, K.C., Duke, S.O., 1981. Tissue localization of polyphenol oxidase in Sorghum. Protoplasma 108, 319–327.

Vaughn, K.C., Duke, S.O., 1984. Function of polyphenol oxidase in higher plants. Function of polyphenol oxidase in higher plants. Physiol. Plantarum 60, 106–112.

Wind, J., Smeekens, S., Hanson, J., 2010. Sucrose: metabolite and signaling molecule. Phytochem 71, 1610–1614.

Yamaki, S., Kajiwara, I., Omura, M., Matsuda, K., 1977. Watercore in Japanese pear (*Pyrus serotina Rehder var*. 'Culta' Rehder). III. Changes in the activities of some enzymes relating to the degradation of cell walls and the accumulation of sugar. Sci. Hortic. 6, 45–53.